Finite-temperature magnetism of CrTe and CrSe

Finite-temperature magnetism of CrTe and CrSe

S Polesya[1], S Mankovsky[1], D Benea[2], H Ebert[1] and W Bensch[3]

[1] Department Chemie und Biochemie, Universität München, Butenandtstraße 5-13,
D-81377 München, Germany
[2] Faculty of Physics, Babes-Bolyai University, 400058 Cluj-Napoca, Romania
[3] Institut für Anorganische Chemie, Christian-Albrechts-Universität zu Kiel,
Max-Eyth-Straße 2, D-24118 Kiel, Germany

Abstract
An investigation on the electronic and magnetic properties of NiAs-type CrTe and CrSe has
been performed for ferromagnetic, antiferromagnetic and non-collinear spin configurations,
using the spin-polarized relativistic KKR (Korringa–Kohn–Rostoker) band structure method.
Calculated exchange coupling parameters, as well as the total energy calculated as a function of
the tilt angle of magnetic moments, indicate the presence of a non-collinear spin structure in
CrTe and CrSe. The existence of a non-collinear spin structure is also shown by Monte Carlo
(MC) simulations used for studies on the temperature dependent magnetization. The results are
compared with available results in the literature and are in satisfactory agreement with the
experimental results.

(Some figures in this article are in colour only in the electronic version)

1. Introduction

Transition-metal chalcogenides have attracted much interest in the past due to their large variety of physical properties, particularly concerning the relationship between the magnetic ordering and the composition.

The system $Cr_{1-x}(Te, Se)$ can be found in different crystallographic structures, depending on the concentration x as well as on the ratio Te:Se. The first x-ray study on CrTe was performed by Haraldsen and Neuber [1], reporting a mixing of two intermediate phases (an α hexagonal phase and a β monoclinic phase). According to the phase diagram determined by Ipser *et al* [2], the system has the hexagonal NiAs structure for $x \leqslant 0.1$. One should note that the stoichiometric CrTe system with NiAs structure does not exist [3]. $Cr_{1-x}Te$ with the hexagonal NiAs structure is a ferromagnet with a Curie temperature $T_C \sim 340$ K, an experimental saturation moment m_s of about 2.4–2.7 μ_B at 4.2 K and an effective paramagnetic moment m_c of $\sim$4.0–4.5 μ_B [4–7]. There is an apparent discrepancy between the magnetic moments m_c on Cr, of 4 μ_B and higher, deduced from susceptibility measurements in the paramagnetic regime, band structure calculations and the low values of Cr magnetic moments m_s obtained from saturation of the magnetization at

4.2 K ($\sim$2.4 μ_B), respectively. If the spin structure in the ferromagnetic (FM) state is assumed to be collinear, the ratio $\alpha = m_c/m_s$ is 4.0/2.4 $\approx$ 1.6. The deviation of this ratio from 1 is quite typical for an itinerant FM system. In fact, inserting the ratio 1.6, together with the Curie temperature, into the Rhodes–Wohlfarth plot [8] the corresponding data point lies quite close to the line representing the average behaviour of itinerant-electron FM solids. On the other hand, a deviation of α from 1 can also be caused to some extent by the presence of a non-collinear spin configuration in the magnetically ordered ground state. The occurrence of such structures has been suggested by various neutron diffraction studies [9–13].

The Curie temperature determined in these experiments is around 370 K. The observed decrease of the total magnetic moment at low temperature in the field-free regime is attributed to the creation of a non-collinear magnetic structure. The transition to the state with non-collinear magnetic structure in CrTe appears at about 170 K [12].

Another compound with interesting magnetic properties which is considered here is CrSe. Tsubokawa [14] and Makovetskii and Shakhlevich [12] reported the para-to antiferromagnetic (AFM) transition in this compound to occur at about 300 K with an effective spin magnetic moment of 4.9 μ_B derived from the measurements of the high-temperature
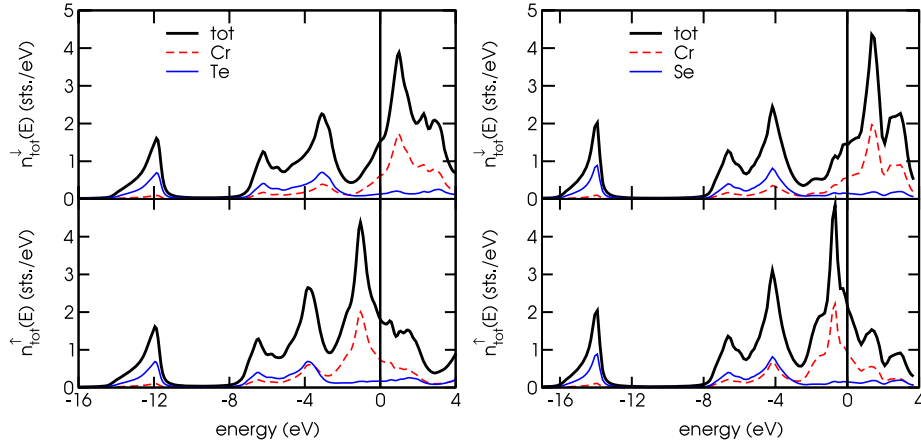
Figure 1. The spin resolved total and component resolved density of states of FM-CrTe (left) and AFM-CrSe (right) calculated by the SPR-KKR method using an optimized lattice parameter (see the text).

susceptibility. Corless *et al* [15] found, from neutron scattering measurements, an umbrella-like AFM spin configuration with a Cr magnetic moment of 4 μ_B.

To clarify this situation the electronic and magnetic properties of stoichiometric CrTe and CrSe have been calculated. Results obtained for the magnetic moments for the ferro- and antiferromagnetic phase are presented in the next sections and compared with data from the literature. To explore the possible presence of a non-collinear spin configuration in the ground state, Monte Carlo (MC) simulations have been performed on the basis of the classical Heisenberg model with the exchange coupling parameters calculated within the KKR Green function method.

2. Band structure calculations

The electronic structure of stoichiometric CrTe and CrSe was calculated self-consistently by means of the spin-polarized relativistic Korringa–Kohn–Rostoker (SPR-KKR) method, employing the atomic sphere approximation (ASA) [16, 17]. The calculation method is based on the KKR–Green function formalism that makes use of multiple scattering theory. The details of the calculational method have been described elsewhere [18, 19]. Exchange and correlation effects were treated within the framework of local spin density functional theory, using the parametrization of Vosko *et al* [20].

The band structure calculations have been performed for the NiAs-type structure (space group $P6_3/mmc$) with the Cr atoms at sites $(0, 0, 0)$ and $(0, 0, \frac{1}{2})$ and Te(Se) atoms at the sites $(\frac{1}{3}, \frac{2}{3}, \frac{1}{4})$ and $(\frac{2}{3}, \frac{1}{3}, \frac{3}{4})$. The lattice parameter *a* was optimized within the total energy calculations keeping the ratio c/a fixed to the experimental value [21]. The calculations have been performed for both FM and AFM magnetic structures of both compounds. The optimized lattice parameters of the different magnetic states (FM and AFM) of CrTe and CrSe differ by less than 1%. Thus, in the subsequent calculations the lattice parameters for stoichiometric compounds (CrTe and CrSe), as well as for Cr(Te, Se) alloys, have been chosen as the ones obtained by lattice optimization: for the FM state of

CrTe- and Te-rich alloys and for the AFM state of CrSe- and Se-rich alloys.

The total and component resolved density of states (DOS) for ferromagnetic CrTe and antiferromagnetic CrSe obtained by the SPR-KKR calculations are shown in figure 1. They are very similar to the results obtained by using the scalar relativistic version of the ASW band structure method [22, 23]. The well-separated narrow energy bands at binding energies around 12 eV and 14 eV have dominating anion (Te and Se, respectively) s character, whilst the higher energy bands have a mixed Cr(3d)–Te(5p) or Cr(3d)–Se(4p) character in CrTe and CrSe, respectively. In the lower part of the d–p band, the p character is stronger and the influence of the exchange-splitting is accordingly of minor importance. The higher part of the d–p band, on the other hand, shows a clear exchange-splitting due to its dominant Cr(3d) character.

The magnetic moments obtained in our calculations are shown in table 1, together with the results reported by Dijkstra *et al* [22]. We present here the results both for the FM and AFM configurations of the investigated compounds, with the Cr spin moments oriented along the *c* axis. The difference between the magnetic moments is very small for the two (FM and AFM) spin configurations considered. This means that they adequately satisfy the assumptions underlying the application of the Heisenberg model, which requires spin magnetic moments to be unchanged under rotation (RSA: rigid spin approximation). Therefore, the RSA model approach can be considered as a reliable basis to study the temperature dependent magnetic properties of CrTe and CrSe compounds.

The spin magnetic moment of Cr obtained within the present calculations is somewhat lower than the value based on ASW calculations, both for FM and AFM configurations. This is a result of the use of optimized lattice parameters ($a = 7.25$ au and $a = 6.7$ au for CrTe and CrSe, respectively) in the present calculations, which are smaller than the experimental values ($a = 7.56$ au and $a = 6.96$ au for CrTe and CrSe, respectively) [4–7], while the calculations of Dijkstra *et al* have been done using the experimental lattice parameters. The total energy calculations show the stability of the FM state for CrTe compared to the AFM one ($\Delta_{FM-AF} = -2.84$ mRyd), while

Table 1. Spin and orbital magnetic moments in CrTe and CrSe resulting from SPR-KKR and ASW [22] calculations done using slightly different lattice parameters (see the text).

	Ferromagnetic			Antiferromagnetic		
	SPR-KKR		ASW	SPR-KKR		ASW
	Spin	Orb.	Spin	Spin	Orb.	Spin
CrTe						
Cr magnetic moment (μ_B)	2.71	0.002	3.51	2.72	0.03	3.17
Te magnetic moment (μ_B)	−0.032	−0.011	0.22	0.00	0.00	—
CrSe						
Cr magnetic moment (μ_B)	2.51	−0.002	3.40	2.52	−0.001	3.0
Se magnetic moment (μ_B)	−0.008	−0.004		0.00	0.00	—

for CrSe the AFM state has a lower energy than the FM one ($\Delta_{\mathrm{FM-AF}} = 3.71$ mRyd).

3. Magnetic exchange coupling parameters

In general, band structure calculations for magnetic systems are performed assuming a collinear magnetic structure. Mapping the results of *ab initio* calculations onto a model Hamiltonian allows one to study non-collinear magnetic structures in materials, as well as their temperature dependent behaviour, in a relatively easy way. However, one should keep in mind the approximations used in this approach when resulting theoretical magnetic structures are compared with those obtained by experiment. The model investigations done in the present work are based on the effective Heisenberg Hamiltonian

$$H_{\mathrm{ex}} = -\sum_{\substack{ij \\ (i \neq j)}} J_{ij} \hat{e}_i \cdot \hat{e}_j, \qquad (1)$$

where the summation is performed over all lattice sites i and j with $i \neq j$. Here $\hat{e}_i$ and $\hat{e}_j$ are the unit vectors along the directions of the magnetic moments on sites i and j respectively, and J_{ij} is the exchange coupling parameter for the corresponding pair of magnetic moments.

A rigorous expression for the exchange parameters J_{ij} can be obtained within local spin density functional (LSDF) theory using the KKR Green function formalism. The approach described by Lichtenstein [24, 25] is based on the calculation of the variation of the total energy with small deviations of two magnetic moments from their equilibrium directions. The exchange interaction parameter J_{ij} between the magnetic moments located on sites i and j is then given by the formula:

$$J_{ij} = \frac{1}{4\pi} \Im \int^{E_F} \mathrm{Tr}_L (t_{i\uparrow}^{-1} - t_{i\downarrow}^{-1}) \hat{\tau}_\uparrow^{ij} (t_{j\uparrow}^{-1} - t_{j\downarrow}^{-1}) \hat{\tau}_\downarrow^{ji} \, \mathrm{d}E. \qquad (2)$$

Here $t_{im_s}^{-1}$ and $\hat{\tau}_{m_s}^{ij}$ are the inverse single-site scattering t-matrix and the scattering path operator for spin orientation $m_s(\uparrow, \downarrow)$ and connected with the sites i and j. Tr_L means the trace over the orbital states labelled by the combined quantum number $L = (l, m_l)$.

The parameters J_{ij} describing exchange coupling between Cr atoms occupying the same sub-lattice, as well as different Cr sub-lattices (see figure 2), in CrSe and CrTe are presented
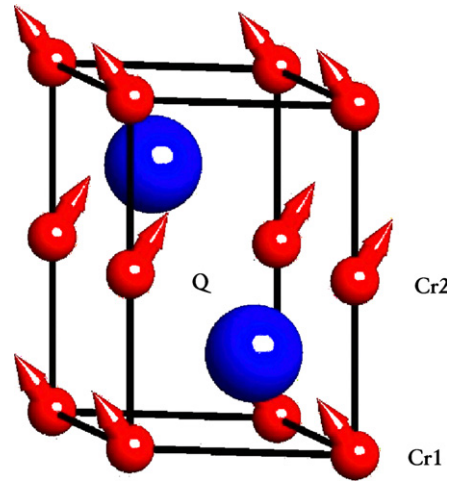

Figure 2. NiAs-like unit cell of CrQ (Q = Te, Se) showing the two Cr sub-lattices Cr1 and Cr2. The arrows indicate the Cr moments tilted by $\pm\theta/2$ away from the *c*-axis, respectively, as assumed for the total energy calculations for non-collinear structures.

in figure 3. They are obtained for collinear spin configurations having the lowest energy, i.e. for the FM order in CrTe and the AFM order in CrSe. Note that the sign of the Cr1–Cr2 exchange coupling parameters calculated for the AFM structure of CrSe via equation (2) has been reversed to conform with the sign convention in equation (1).

For both compounds the exchange coupling parameters have an oscillatory behaviour with a rather slow decay with the inter-site distance R_{ij}. As was shown by Hirone and Adachi [26], this behaviour is typical for the exchange parameters in systems having the NiAs-type lattice structure. The resulting competition between the oscillating ferromagnetic and antiferromagnetic exchange should lead to complex spin configurations, including frustration and non-collinear magnetic order in these systems [27, 28].

4. Non-collinear spin structure

To give a clear indication concerning the most stable spin configuration, one can perform either band structure calculations for a non-collinear spin arrangement in the CrTe and CrSe compounds, or MC simulations using the exchange
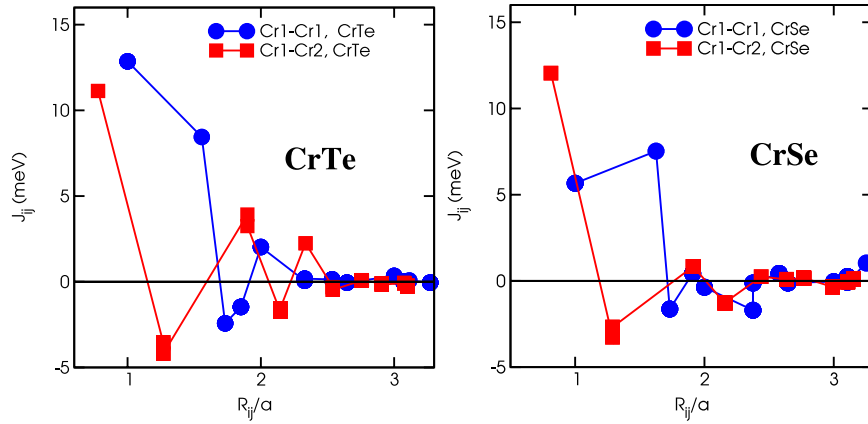
Figure 3. Cr–Cr exchange coupling parameters J_{ij} obtained for the FM spin configuration in CrTe (left) and the AFM spin configuration in CrSe (right) as a function of the inter-site distance R_{ij} (a is the optimized lattice parameter).
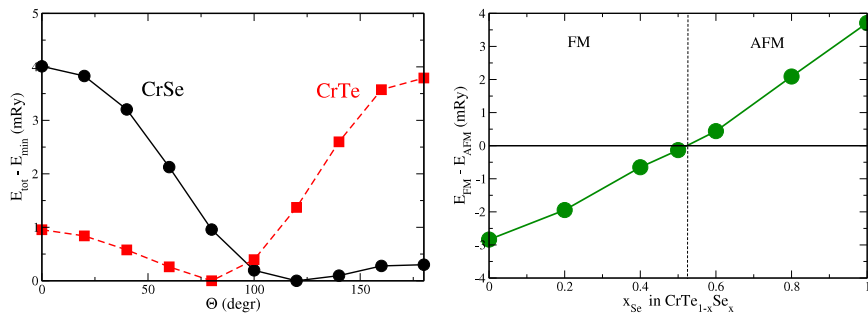

Figure 4. Left panel: total energy of CrSe and CrTe as a function of the tilt angle θ for the Cr magnetic moments (see figure 2). Right panel: difference in total energy between the FM and AFM states of $CrTe_{1-x}Se_x$ as a function of Se concentration.

coupling parameters evaluated within *ab initio* calculations for a collinear magnetic structure. The first way should give more precise results but requires considerable computational effort. Therefore, we performed self-consistent calculations only for the non-collinear spin configuration, keeping the translational symmetry of the lattice unchanged (figure 2), in order to prove the instability of the collinear spin configuration. Tilting the Cr1 and Cr2 magnetic moments by the angles $\pm\theta/2$, as is shown in figure 2, we calculated the dependence of the total energy on the tilt angle θ between the spins. The results for CrTe and CrSe are shown in the left panel of figure 4.

It can clearly be seen that the FM spin configuration (with $\theta = 0°$) is more stable in the case of CrTe than the AFM ($\theta = 180°$) configuration, while for CrSe the situation is reversed. As is seen in the right panel of figure 4, the difference between the energies in FM and AFM states, $E_{FM} - E_{AFM}$, for the alloys $CrTe_{1-x}Se_x$ varies nearly linearly as a function of Se content, from -2.84 mRyd for CrTe to $\approx +3.71$ mRyd for CrSe.

However, for CrTe and CrSe, the FM and AFM phases are not the most stable ones. The lowest energy corresponds to a tilt angle of $\theta = 80°$ and $\theta = 120°$ between the Cr1 and Cr2 moments in the case of CrTe and CrSe, respectively. Although these results confirm the expectation that the ground state spin configuration of these compounds is non-collinear, they do not rule out the existence of other energetically more favourable non-collinear spin structures.

Indeed, more favourable spin structures were found within MC simulations based on the Heisenberg model, using a standard Metropolis algorithm [29]. The exchange coupling parameters were calculated within the KKR Green function formalism, as mentioned above. The critical temperature has been evaluated using the cumulant crossing method [29]. The largest cell used in simulations consists of $12 \times 12 \times 12$ unit cells (3456 atoms) that were repeated with periodic boundary conditions. The simulations have been performed under cooling of a sample starting at a high-temperature paramagnetic state. In the case of CrTe, a phase transition to a state with dominantly collinear configuration (FM) was observed around the temperature 280 K. The temperature of this transition (T_C) is in reasonably good agreement with that obtained in experiment (350 K [12], 320 K [14]). A further temperature decrease is accompanied by a slow increase of the total magnetic moment. Note, however, that the FM-like ordering is very sensitive to the number of atomic shells taken into account for the energy evaluation within the MC simulation, because of the rather slow decay of the exchange coupling parameters with distance (see figure 3). Therefore, we to into account in our simulations all couplings within a sphere with radius $R_{max} = 3.3a$, with a the lattice parameter. A further decrease of the temperature leads to another phase transition at $T \approx 30$ K. The magnetic state below this temperature is characterized by a small effective total magnetic moment. This is caused by the non-collinear magnetic
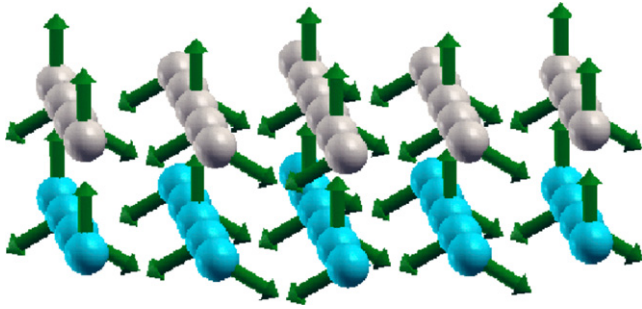
Figure 5. Spin spirals created at low temperature within the xy plane of the Cr sub-lattice in the CrTe compound having a NiAs structure; different colours show nonequivalent atoms in the unit cell.

structure, shown in figure 5, which consists of a set of spin spirals within the xy-planes of the Cr sub-lattice in CrTe. The transition temperature to the non-collinear magnetic state is small when compared to that observed in experiment. This discrepancy can be attributed to the approximations used within the present model considerations, such as the conditions for calculating the exchange coupling parameters, the number of atomic shells accounted for in the MC simulations, use of the experimental c/a ratio instead of that found within structure optimization procedure, etc.

The MC simulations for CrSe show a transition to the ordered magnetic structure at 280 K, which is shown in figure 6. As is seen, the z-components of the Cr1 and Cr2 magnetic moments are aligned anti-parallel to each other, however the x and y components are non-zero due to an umbrella-like magnetic structure in the system, which is also observed in experiment [15]. Note that

the magnetic structure obtained within the MC simulations exhibits a non-compensated total magnetic moment $\approx 0.6 \mu_B$, i.e. one can speak about non-collinear ferrimagnetism of CrSe. Previous authors [14, 15, 30] discuss a transition to a non-collinear AFM state on the basis of their experimental work. The corresponding transition temperature (320 K) found theoretically within the present work is in good agreement with that observed experimentally (280 K [30], 360 K [14], 300 K [15]). Figure 6 (top right) represents the magnetic structure within the basal Cr planes. One can clearly see that this structure leads to an enlarged magnetic unit cell within the plane with a period $a\sqrt{3}$, while the period along the z direction remains unchanged. This is in full agreement with the results of a neutron scattering experiment [15].

The origin of the observed magnetic structure can be traced back to the exchange coupling parameters. We can restrict the consideration to the J_{ij} parameters characterizing the interactions between the Cr1 and Cr2 sub-lattices (see figure 2). As is seen in figure 3, the exchange interaction between the first neighbouring atoms of Cr1 and Cr2 sub-lattices is strongly ferromagnetic (CrTe: ≈ 11.1 meV; CrSe: ≈ 12.1 meV) while the next-neighbouring Cr1 and Cr2 atoms couple antiferromagnetically (CrTe: ≈ -3.7 meV, CrSe: ≈ -3 meV). Accounting for the number of atoms in these two shells (first neighbours—2 atoms, second neighbours—12 atoms), their contribution results in AFM ordering of Cr1 and Cr2 atoms, both for CrSe and CrTe. However, accounting for the other long-range exchange interactions leads to non-collinear structures with AFM alignment of Cr1 and Cr2 sub-lattices in CrSe and a more preferable FM alignment of Cr1 and Cr2 sub-lattices in CrTe. The reason for this difference is the stronger FM couplings at large distances between Cr1 and Cr2
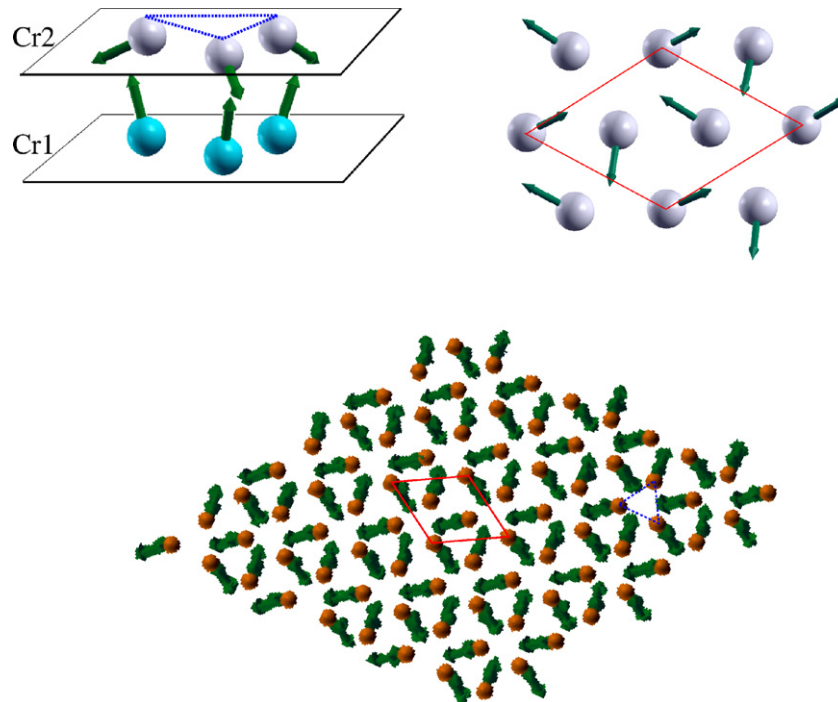

Figure 6. Umbrella-like structure created in CrSe by Cr1 and Cr2 sub-lattices (top left). Projection of the unit cell of CrSe on the xy basal plane (top right). An enlargement of the unit cell is observed due to magnetic superstructure (solid line) and the umbrella-like cell (dashed line) are shown at the bottom.
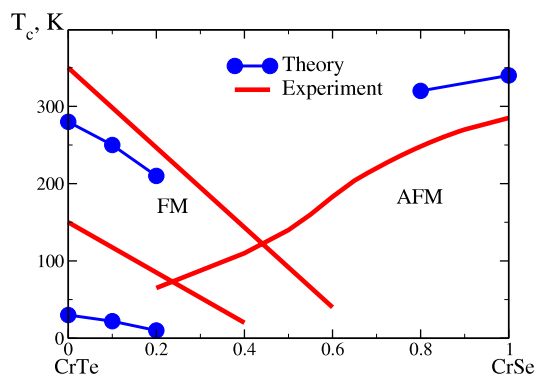
Figure 7. Magnetic phase diagram for the CrTe$_{1-x}$Se$_x$ system. Theoretical results obtained in the present work are compared with the results of experiment [12].

atoms in CrTe than in CrSe; these stabilize the FM alignment of the Cr1 and Cr2 sub-lattices in CrTe. As was mentioned above, a competition between all FM and AFM interactions, both within the Cr1 and Cr2 sub-lattices as well as between them, leads to the non-collinearity in these systems.

Substitution of Te atoms by Se in CrTe, and substitution of Se atoms by Te in CrSe, results in modifications of the exchange interactions between Cr atoms leading to concentration dependent critical temperatures in CrTe$_{1-x}$Se$_x$ alloys. The occupation of the chalcogenide sub-lattice, in this case by Te and Se atoms, was assumed to be completely random. This situation was accounted for by making use of the CPA alloy theory [31, 32]. In combination with the KKR band structure formalism it allowed us to study the electronic and magnetic properties of the ground state of CrTe$_{1-x}$Se$_x$ alloys at $T = 0$ K. The finite-temperature magnetic properties, as well as in the case of stoichiometric compounds, have been studied using Monte Carlo (MC) simulations based on the classical Heisenberg model.

The results and corresponding data are presented by the phase diagram shown in figure 7, where theoretical critical temperatures for Te- and Se-rich alloys are compared with experimental results. As one can see, the approach used in the present work leads to a satisfactory agreement with experimental data. In the mid region of concentrations the experimental phase diagram becomes more complex. On the other side, the calculated magnetic structure becomes very sensitive to small variations of the exchange parameters, leading to non-collinear structures in the alloys.

5. Conclusions

Self-consistent SPR-KKR calculations for CrTe and CrSe show an instability of the collinear magnetic states for both compounds. Within MC simulations for CrTe, two phase transitions have been obtained upon a temperature increase— at $T = 30$ K—from the non-collinear to the FM state and at $T = 280$ K—from the FM to the PM state. In CrSe the MC simulation shows a so-called umbrella-like structure below $T = 320$ K, with anti-parallel alignment of the magnetic moments of neighbouring layers. All these results are in satisfactory agreement with the experimental data of various authors.

References

[1] Haraldsen H and Neuber A 1937 *Z. Anorg. Allg. Chem.* **234** 353
[2] Ipser H, Komarek K L and Klepp K O 1983 *J. Less-Common Met.* **92** 265
[3] Berg A 1950 *PhD Thesis* University of Oslo
[4] Lotgering F K and Gorter E W 1957 *J. Phys. Chem. Solids* **3** 238
[5] Oshawa A, Yamaguchi Y, Kazama N, Yamaguchi H and Watanabe H 1972 *J. Phys. Soc. Japan* **33** 1303
[6] Hirone T and Chiba S 1960 *J. Phys. Soc. Japan* **15** 1991
[7] Ohta S 1985 *J. Phys. Soc. Japan* **54** 1076
[8] Rhodes P and Wohlfarth E P 1963 *Proc. R. Soc.* A **273** 247
[9] Bertaut E F, Roult G, Aleonard R, Pauthenet R, Chevreton M and Jansen R 1964 *J. Physique* **25** 582
[10] Lambert-Andron B, Grazhdankina N P and Vettier C 1979 *J. Physique* **39** L43
[11] Andresen A F 1963 *Acta Chem. Scand.* **17** 1335
[12] Makovetskii G I and Shakhlevich G M 1979 *Krist. Tech.* **14** 97
[13] Hamasaki T, Hashimoto T, Yamaguchi Y and Watanabe H 1975 *Solid State Commun.* **16** 895
[14] Tsubokawa I 1956 *J. Phys. Soc. Japan* **11** 662
[15] Corless I M, Elliott N, Hartings J M and Sass R I 1961 *Phys. Rev.* **122** 1402
[16] Korringa J 1947 *Physica* **13** 392
[17] Kohn W and Rostoker N 1954 *Phys. Rev.* **94** 1111
[18] Ebert H 2000 *Electronic Structure and Physical Properties of Solids* vol 535, ed H Dreyssé (Berlin: Springer) p 191
[19] Ebert H *et al* 2002 *The Munich SPR-KKR Package, Version 2.1.1* http://olymp.cup.uni-muenchen.de/ak/ebert/SPRKKR
[20] Vosko S H, Wilk L and Nusair M 1980 *Can. J. Phys.* **58** 1200
[21] Chevreton M, Bertaut E F and Jellinek F 1963 *Acta Crystallogr.* **16** 431
[22] Dijkstra J, Bruggen C F, Haas C and de Groot R A 1989 *J. Phys.: Condens. Matter* **1** 9163
[23] Dijkstra J, Weitering H H, Bruggen C F, Haas C and de Groot R A 1989 *J. Phys.: Condens. Matter* **1** 9141
[24] Liechtenstein A I, Katsnelson M I, Antropov V P and Gubanov V A 1987 *J. Magn. Magn. Mater.* **67** 65
[25] Liechtenstein A I, Katsnelson M I and Gubanov V A 1984 *J. Phys. F: Met. Phys.* **14** L125
[26] Hirone T and Adachi K 1957 *J. Phys. Soc. Japan* **12** 156
[27] Vleck J H V 1951 *J. Phys. Radium* **12** 262
[28] Smart J S 1952 *Phys. Rev.* **86** 968
[29] Binder K 1997 *Rep. Prog. Phys.* **60** 487
[30] Makovetskii M I 1986 *Sov. Phys.—Solid State* **28** 447
[31] Soven P 1987 *Phys. Rev.* **156** 809
[32] Stocks G M, Temmerman W and Györffy B L 1980 *Phys. Rev. Lett.* **41** 1200